Effects of a Mismatch in the In-phase and In-quarature Paths, and of phase noise, in QDCPSK-OFDM Modems[1]

M.Gabriella Di Benedetto, Paolo Mandarini, and Lorenzo Piazzo (authors are in alphabetical order)
Universita' degli Studi di Roma "La Sapienza"
Dipartimento INFOCOM, via Eudossiana 18, 00184 Rome, Italy.
tel:39-6-44585483;fax:39-6-4873300
e-m: gaby@acts.ing.uniroma1.it, paolo@acts.ing.uniroma1.it, lorenz@acts.ing.uniroma1.it

Abstract

In digital systems operating at very high bitrate, analog filters must be used in the baseband. A mismatch between the in-phase (I) and in-quadrature (Q) paths may occur. Theoretical analysis shows that the mismatch can be represented by a unique mismatch transfer function, in which the effects of the mismatch in the transmitter and receiver side add up; results are reported on the mismatch produced by the inaccuracy of the poles position of RLC Butterworth filters. In addition, the effect of phase noise on the system performance is evaluated.

Introduction

In digital systems operating at very high bitrate, the baseband shape must be realized by analog filters; a filter mismatch problem arises in the in-phase (I) and in-quadrature (Q) paths. The aim of the present paper is to extend the analysis of a previous paper [1] which examined the mismatch of the analog filters, and phases of the carriers, in the I and Q paths of the transmitter. The present analysis includes the receiver and the effects of the phase noise introduced by local oscillators. In section 1, the performance of a QDCPSK-OFDM system is summarized. In the section 2, the SNR worsening due to the TX and RX mismatch is evaluated. The mismatch can be originated by an inaccuracy in the position of the poles: Butterwoorth filters are considered in section 3. Phase noise originated in the local oscillators cause degradation of system performance. Previous investigators analyzed the effect of phase noise on OFDM systems ([3], [4]). In the present paper, a full-digital QDCPSK-OFDM system is considered. The impact of phase noise is theoretically analysed, and the SNR worsening is evaluated in section 4. In section 5, quantitative results for some phase noise spectra are presented, and compared with simulations results in order to validate the theorical analysis. Finally, section 6 contains the conclusions.

Section I - Performance evaluation of a QDCPSK OFDM system.

Figure 1 depicts the block diagram of a DCQPSK/OFDM modem; N is the dimension of the FFT and IFFT processors (N=512 in the MEDIAN project); $M_1+M_2+1 = N_u$ is the number of used subcarriers (M_1, M_2, is the number of subcarriers at frequencies below and above the system carrier respectively, with frequency spacing $\Delta f=1/T_o$), $\{p_{-M_1}, ..., p_o, ..., p_{M_2}\}$ and $\{q_{-M_1-1}, ..., q_o, ..., q_{M_2}\}$, $|q_j|=|p_j|=1$, are the constellation points, before and after the differential encoder, each point p_j, from $-M_1$ to M_2, carrying a two-bit data symbol; $B=N\cdot\Delta f$ is the frequency of the system clock; $T = T_o+T_g$ is the OFDM symbol duration, where T_g is the guard time; $\psi(t)$ is the phase noise with a power spectral density $N_\psi(f)$; $n(t)$ is the low-pass equivalent of the thermal noise modeled as a complex gaussian process, with two-side spectral power density $4N_o$, where N_o represent the RF two-side spectral density. The Signal to Noise Ratio is $SNR = P_R/2\ N_o f_s$, where P_R is the received power and f_s is the effective on air symbol rate.

With reference to figs.1 and 2, define:

$G_{BTI}(f) = (\sin\pi fT/\pi f)\cdot H_{BTI}(f) \equiv G^*_{BTI}(-f)$: BB TX transfer function of the I path

$G_{BTQ}(f) = (\sin\pi fT/\pi f)\cdot H_{BTQ}(f) \equiv G^*_{BTQ}(-f)$: BB TX transfer function of the Q path

$H_{BRI}(f) \equiv H^*_{BRI}(-f)$: BB TR filter in the I path $H_{BRQ}(f) \equiv H^*_{BRQ}(-f)$: BB TR filter in Q path

ϕ: phase mismatch between the TX I and Q carriers θ: phase mismatch between the RX I and Q carriers

$H(f)$: low-pass equivalent transfer function of the IF and RF sections of the transmitter, channel and receiver.

γ_k: precorrection factor which multiplies int q_m to produce the on-air amplitude c_m (i.e. $c_m = q_m\cdot\gamma_m$) of $f_k = k\ \Delta f$

From the precorrected $\{c_m\}$, the S/P converter generates N complex D_k, $k = 0,..,N-1$, which the IFFT processor uses to generate a periodic complex sequence d_k, where:

---

[1] This work was partly funded by the European Union under project ACTS-MEDIAN #006

$$d_k = \text{IFFT of } \{D_m\} = \sum_{m=0}^{N-1} D_m e^{j2\pi\frac{mk}{N}} \text{ periodic of period } N \qquad D_m = \begin{cases} c_m & 0 \le m \le M_1 \\ 0 & M_1 < m \le N - M_2 \\ c_{m-N} & N - M_2 < m \le N-1 \end{cases}$$

In absence of a mismatch, one has:

$$G_{BTI}(f) = G_{BTQ}(f) \equiv G_{BT}(f) \qquad H_{BRI}(f) = H_{BRQ}(f) \equiv H_{BR}(f) \quad \phi = \theta = 0 \tag{1}$$

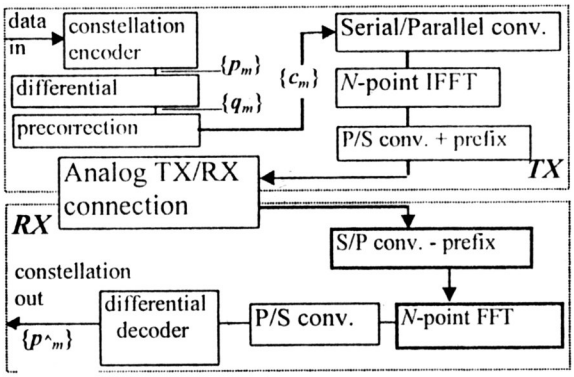

Figure 1 Block diagram of an OFDM modem.

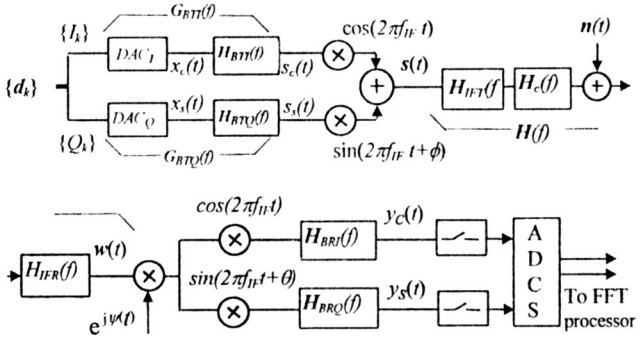

Figure 2 Block diagram of the baseband equivalent of the analog TX/RX connection.

and the relationship between the transmitted and the received m-th constellation point p_m is:

$$\hat{p_m} = p_m \cdot \left[G_o^*(f_{m-1})\gamma_{m-1}^* \cdot G_o(f_m)\gamma_m \right] \equiv p_m \cdot \beta_m \tag{2}$$

where: $G_o(f) = G_{BT}(f) \cdot H(f) \cdot H_{BR}(f)$ (3)

i.e., the presence of the TX and RX filters produce a multiplicative (complex) bias which can be totally removed by using a precorrection factor [i.e.: $\gamma_m = 1/G_o(f_m)$] before the IFFT processor (the bias produced by the channel transfer function $H(f)$ cannot be removed by the precorrection factors). The BER is given by:

$$BER = \frac{1}{2} erfc\{y\} \qquad y^2 = \frac{SNR}{4 \cdot (1 + T_g / T_o)} \tag{4}$$

Section II – Effects of a TX-RX mismatch

Figure 2 shows the TX and RX; $\{d_{-N_g}, \ldots, d_{N-1}\}$ is splitted into $\{I_{-N_g}, \ldots, I_{N-1}\}$ and $\{Q_{-N_g}, \ldots, Q_{N-1}\}$ which are separately D to A converted, filtered and cos/sin modulated. The input to the first IF-TX filter is:

$$\begin{aligned} s(t) &= s_c(t) \cdot \cos(2\pi \ f_{IF} t) - s_s(t) \cdot sin(2\pi \ f_{IF} t + \phi) \equiv s_I(t) \cdot \cos(2\pi \ f_{IF} t) - s_Q(t) \cdot sin(2\pi \ f_{IF} t) \\ s_I(t) &= s_c(t) - sin\phi \cdot s_s(t) \\ s_Q(t) &= \cos\phi \cdot s_s(t) \\ s_c(t) &= \sum_{k=-N_g}^{N-1} I_k \cdot g_{BTI}(t - k/B) \ g_{BTI}(t) \Leftrightarrow G_{BTI}(f) \\ s_s(t) &= \sum_{k=-N_g}^{N-1} Q_k \cdot g_{BTQ}(t - k/B) \ _{BTQ}(t) \Leftrightarrow G_{BTQ}(f) \end{aligned} \tag{5}$$

Its complex envelope is $s(t) = s_I(t) + js_Q(t) \Leftrightarrow S(f)$. Let $w(t) = w_c(t) + jw_s(t) \Leftrightarrow W_c(f) + jW_s(f)$ indicate the complex envelope of the output of the receiver IF filter. One has:

$$W_c(f) = \frac{1}{2}\left\{ \left[G_{TI}(f) + G_{TI}^*(-f) \right] \cdot \sum_{k=-N_g}^{N-1} I_k \cdot e^{-j2\pi fk/B} + j \cdot \left[G_{TQ}(f) - G_{TQ}^*(-f) \right] \cdot \sum_{k=-N_g}^{N-1} Q_k \cdot e^{-j2\pi fk/B} \right\} \tag{6}$$

$$W_s(f) = \frac{1}{2j}\left\{ \left[G_{TI}(f) - G_{TI}^*(-f) \right] \cdot \sum_{k=-N_g}^{N-1} I_k \cdot e^{-j2\pi fk/B} + j \cdot \left[G_{TQ}(f) + G_{TQ}^*(-f) \right] \cdot \sum_{k=-N_g}^{N-1} Q_k \cdot e^{-j2\pi fk/B} \right. \tag{7}$$

where:

$$\begin{aligned} G_{TI}(f) &\equiv G_{BTI}(f) \cdot H(f) \\ G_{TQ}(f) &\equiv e^{j\phi} \cdot G_{BTQ}(f) \cdot H(f) \end{aligned} \tag{8}$$

After demodulation and LP filtering, the Fourier Transform of the I and Q components $y_c(t)$ and $y_s(t)$ is:

$$\begin{aligned} y_c(t) &= w_c(t) * h_{BRI}(t) \Leftrightarrow Y_c(f) = W_c(f) \cdot H_{BRI}(f) \\ y_s(t) &= \left[w_s(t) \cdot cos\theta - w_c(t) \cdot sin\theta \right] * h_{BRQ}(t) \Leftrightarrow Y_s(f) = H_{BRQ}(f) \cdot \left[W_s(f) \cdot cos\theta - W_c(f) \cdot sin\theta \right] \\ Y(f) &= Y_c(f) + jY_s(f) = W_c(f) \cdot \left[H_{BRI}(f) - H_{BRQ}(f) \cdot jsin\theta \right] + jW_s(f) \cdot H_{BRQ}(f) \cdot cos\theta \end{aligned} \tag{9}$$

and, defining:

$$G_o(f)=\frac{\left[G_{TI}(f)+G_{TQ}(f)\right]\left[H_{BRI}(f)+e^{-j\theta}H_{BRQ}(f)\right]}{2}+\frac{\left[G_{TI}^{*}(-f)-G_{TQ}^{*}(-f)\right]\left[H_{BRI}(f)-e^{j\theta}H_{BRQ}(f)\right]}{2}=$$
$$\cong\frac{\left[G_{TI}(f)+G_{TQ}(f)\right]\left[H_{BRI}(f)+e^{-j\theta}H_{BRQ}(f)\right]}{2} \tag{10}$$

$$G_e(f)=\frac{\left[G_{TI}(f)-G_{TQ}(f)\right]\left[H_{BRI}(f)+e^{-j\theta}H_{BRQ}(f)\right]}{2}+\frac{\left[G_{TI}^{*}(-f)+G_{TQ}^{*}(-f)\right]\left[H_{BRI}(f)-e^{j\theta}H_{BRQ}(f)\right]}{2} \tag{11}$$

one obtains:

$$Y(f)=G_o(f)\sum_{k=-N_g}^{N-1}(I_k+jQ_k)\cdot e^{-j2\pi fk/B}+G_e(f)\sum_{k=-N_g}^{N-1}(I_k-jQ_k)\cdot e^{-j2\pi fk/B}=$$
$$=G_o(f)\cdot\left\{\sum_{k=-N_g}^{N-1}D_k\cdot e^{-j2\pi fk/B}+H_e(f)\cdot\sum_{k=-N_g}^{N-1}D_k^{*}\cdot e^{-j2\pi fk/B}\right\} \tag{12}$$

where:

$$H_e(f)\equiv\frac{G_e(f)}{G_o(f)}\cong\frac{\left[G_{TI}(f)-G_{TQ}(f)\right]\cdot\left[H_{BRI}(f)+e^{-j\theta}H_{BRQ}(f)\right]+\left[G_{TI}^{*}(-f)+G_{TQ}^{*}(-f)\right]\cdot\left[H_{BRI}(f)-e^{j\theta}H_{BRQ}(f)\right]}{\left[G_{TI}(f)+G_{TQ}(f)\right]\cdot\left[H_{BRI}(f)+e^{-j\theta}H_{BRQ}(f)\right]}$$
$$=\frac{\left[H_{HBI}(f)-e^{j\phi}H_{HBQ}(f)\right]}{\left[H_{HTI}(f)+e^{j\phi}H_{HBQ}(f)\right]}+\frac{\left[H_{BRI}(f)-e^{j\theta}H_{BRQ}(f)\right]}{\left[H_{BRI}(f)+e^{-j\theta}H_{BRQ}(f)\right]}\frac{H^{*}(-f)}{H(f)}\equiv H_{eT}(f)+H_{eR}(f) \tag{13}$$

Eq.(13) shows that the transmitter and the receiver mismatches contribute to $H_e(f)$ *in an additive form*; in particular, the contribution to $H_e(f)$ of the transmitter mismatch is given by:

$$H_{eT}(f)=\left[H_{BTI}(f)-e^{j\varphi}H_{BTQ}(f)\right]/\left[H_{BTI}(f)+e^{j\varphi}H_{BTQ}(f)\right] \tag{14}$$

and the similar contribution due to the receiver is:

$$H_{eR}(f)=\frac{\left[H_{BRI}(f)-e^{j\theta}H_{BRQ}(f)\right]}{\left[H_{BRI}(f)+e^{-j\theta}H_{BRQ}(f)\right]}\frac{H^{*}(-f)}{H(f)}\cong\frac{\left[H_{BRI}(f)-e^{j\theta}H_{BRQ}(f)\right]}{\left[H_{BRI}(f)+e^{-j\theta}H_{BRQ}(f)\right]} \tag{15}$$

(the last approximation holds in the case of arithmetic symmetry for $H(f)$, i.e. $H(f) = H^{*}(-f)$).

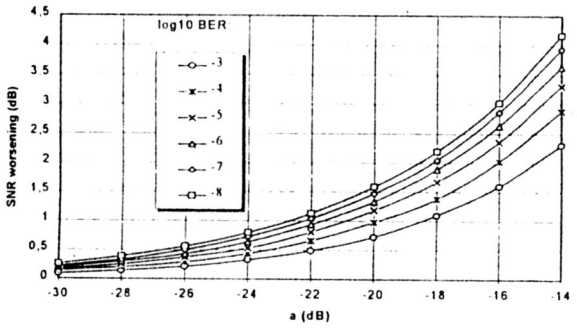

Figure 3. SNR worsening versus a (dB), for different values of $log_{10}(BER)$.

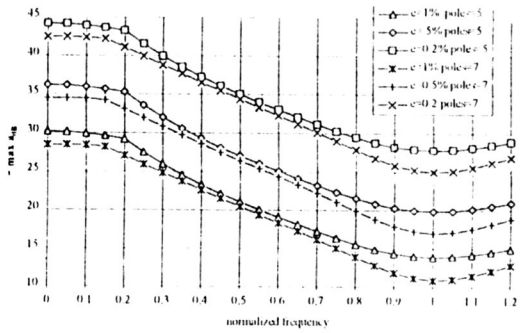

Figure 4. Behavior of a_{dB} maximum over 100 realizations, for different values of number of poles and of the maximum error e in poles position. The I and Q filters are of Butterwoorth type.

Comparing eq.(12) with the eq.(14) of ref.[1], shows that the received signals have the same analytical form but a different definition of H_e; therefore, the considerations carried from (14) of ref.[1] also hold in the present case. In particular, in case of perfect precorrection, the BER can be obtained by averaging the following equation:

$$BER(m;\psi_m,\zeta_m)=\frac{1}{4}erfc(z_{m+})+\frac{1}{4}erfc(z_{m-}) \tag{16}$$
$$z_{m\pm}^2=\frac{SNR}{4(1+T_g/T_o)}\left[1\pm\sqrt{2}a_m(\cos\psi_m+\cos\zeta_m)\right]^2\quad a_m=\left|H_e(f_m)\right|$$

over ψ_m and ζ_m, which can be assumed as random variables uniformly distributed over 0-2π. Figure 3, shows the SNR worsening due to the presence of the I-Q mismatch, represented by the value of a(dB) = $|H_e(f)|$ and for different BER, evaluated in absence of mismatch. Observe that the worsening depends on $|H_e(f)|$, and not on the phase. For example, if a maximum worsening of 2 dB for BER = 10^{-7} can be accepted, fig.1 shows that the

maximum a value is -18 dB. Note that mismatch effects at TX and RX sides, eq.(13), are separable; therefore, if a maximum overall value for a is given, the maximum mismatch is in the worst case: $|H_{eT}(f)|+|H_{eR}(f)| \le a$.

Section III – Mismatch due to poles position inaccuracy: a case study

In many practical situations a BB filter is defined by its zeros z_1, z_2,.. and poles p_1, p_2,... However, if the components inaccuracy is taken into account, the real transfer function of the filter is:

$$H_{Bxy}(f) = \frac{\prod(j2\pi f - z_i - \varepsilon_i)}{\prod(j2\pi f - z_i - \eta_i)} \equiv H_{Bxy}(f;\varepsilon,\eta) \tag{17}$$

which produces a mismatch function given by:

$$H_e(f) \equiv \frac{H_{Bx}(f;\varepsilon,\eta) - H_{Bx}(f;\varepsilon',\eta')}{H_{Bx}(f;\varepsilon,\eta) + H_{Bx}(f;\varepsilon',\eta')} \equiv a(f)\cdot e^{j\theta(f)} \tag{18}$$

Figure 4 shows the maximum of $a_{dB}(f)$ over 100 realizations of a Butterworth low-pass filter with poles allocation affected by random errors uniformly distributed between +/- e, as a function of the normalized frequency, with parameters e, and number of poles. Figure 4 can be combined with Fig. 3. For example, if a 7-pole Butterwoorth with cut-off frequency equal to 0.8 $N\,\Delta f/2$ is used in the TX or RX side, and a worsening of 1 dB on SNR is imposed for $P_e = 10^{-5}$, a value a = -21 dB is required; therefore, it appears that a maximum position error of about 0.5% can be tolerated. If the same filter is present on both sides, each side must contribute for a = -27 dB, and a maximum position error of 0.2 % must be imposed.

Section IV – System analysis in the presence of phase noise

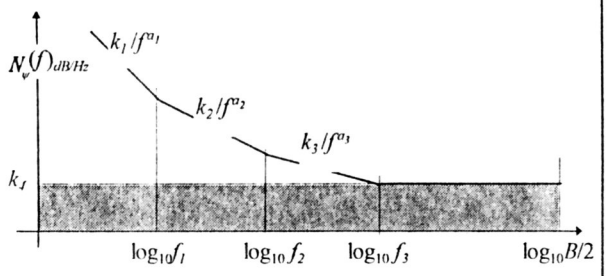

Figure 5. One-sided power spectrum of the phase noise.

LO #	k1	a1	f1 kHz	k2	a2	f2 kHz	k3	a3	f3 MHz
2	4e-5	1.2	10	1.5e-7	0.6	100	1.5e-4	1.2	112.5
1	1e-2	1.5	10	1e-6	0.5	100	1e-6	0.5	112.5

Table 1. Phase noise spectra of two different local oscillators

In the present section, apart from thermal and phase noise, the connection IFFT-FFT is supposed ideal, so that the complex envelope of the received signal, during the current OFDM symbol, is given by:

$$y(t) = e^{j\psi(t)} \sum_{k=-N_g}^{N-1} d_k\, g(t - \frac{k}{B}) + n(t) \tag{19}$$

where $n(t)$ is the thermal noise, $\Psi(t)$ is the phase noise, $g(t)=sen(\pi tB)/(\pi tB)$ and:

$$d_k = IFFT\{D_m\} = \sum_{m=0}^{N-1} D_m e^{j2\pi\frac{mk}{N}}.$$

The received signal is sampled to obtain $N+N_g$ samples from which the prefix is removed; the remaining N samples are FFT transformed to compute an estimate of the transmitted constellation point, given by

$$\hat{D}_h = \frac{1}{N}\sum_{k=0}^{N-1} y(\frac{k}{B}) e^{-j2\pi\frac{kh}{N}} = \frac{1}{N}\sum_{k=0}^{N-1}(d_k e^{j\psi_k} + n_k) e^{-j2\pi\frac{k\cdot h}{N}} = \frac{1}{N}\sum_{m=0}^{N-1}\sum_{k=0}^{N-1} D_m e^{j\psi_k} e^{j2\pi\frac{km}{N}} e^{-j2\pi\frac{kh}{N}} + \frac{1}{N}\sum_{k=0}^{N-1} n_k e^{-j2\pi\frac{kh}{N}} =$$

$$= \sum_{m=0}^{N-1} D_m (\frac{1}{N}\sum_{k=0}^{N-1} e^{j\psi_k} e^{j2\pi\frac{k\cdot(m-h)}{N}}) + v_h = \sum_{m=0}^{N-1} D_m \Psi_{m-h} + v_h = D_h\Psi_0 + \varepsilon_h + v_h \tag{20}$$

where $\Psi_h = \frac{1}{N}\sum_{k=0}^{N-1} e^{j\psi_k} e^{j2\pi\frac{k\cdot h}{N}}$ and $\varepsilon_h = \sum_{m=0, m\neq h}^{N-1} D_m \Psi_{m-h}$.

As a result, from (20), the estimate of D_h is affected by a complex multiplicative bias Ψ_0, by thermal noise v_h, and by Cosymbol Interference (CSI) ε_h. The CSI coefficients Ψ_k are periodic with period N, since they are the

FFT of $e^{j\Psi_k}$; they are random, thus ε_h is a zero mean complex gaussian random variable. Indeed, σ_ε^2 depends upon the symbol detected: unused carriers do not contribute to CSI. Consequently, symbols transmitted on the left or right-most carrier experience half of the CSI experienced by a symbol transmitted on the central carrier; the worst case variance for ε_h, assuming $N_u/2$ used subcarriers above the central frequency and $N_u/2$ used subcarrier below, and that the D_k are independent, is thus:

$$\sigma_\varepsilon^2 = E\{\varepsilon_0 \varepsilon_0^*\} = \sum_{h,k\neq 0} E\{D_{-k} D_{-h}^*\} E\{\Psi_k \Psi_h^*\} = \sum_{\substack{k=-N_u/2 \\ k\neq 0}}^{k=N_u/2} E\{|\Psi_k|^2\} \tag{21}$$

Phase noise adds the CSI component to the thermal noise, and, through the multiplicative bias $\Psi_0 = \Psi e^{j\chi}$, weakens (as it results $E\{\Psi\} < 1$) and rotates the received point estimate by χ rad. The final differential decoder compensates the phase rotation, but doubles the additive noise variance and squares the multiplicative bias; the BER can be approximated as:

$$P_b = \frac{1}{2} erfc\left(\sqrt{\frac{E\{\Psi\}^4}{4(\sigma_\varepsilon^2 + \sigma_\nu^2)}}\right) \tag{22}$$

where the thermal noise variance is linked to the system SNR by $\sigma_\nu^2 = \frac{N + N_g}{N \cdot SNR}$. The SNR worsening, defined as the increase of the SNR which compensates the presence of phase noise is given (in dB) by $W = -10 \cdot log\left(E\{\Psi\}^4 - \sigma_\varepsilon^2 / \sigma_\nu^2\right)$ and can be computed from $E\{\psi\}, \sigma_\varepsilon^2$, and SNR.

Section V – Impact of phase noise on system performance

The phase sequence ψ_k is obtained by sampling the phase signal $\psi(t)$ with a sampling frequency B: therefore, we can consider its aliased power spectrum as band-limited between $-B/2$ and $B/2$. Usually (e.g. [2], sec.10), the two-sided power spectrum $N_\psi(f)$ of the phase noise $\psi(t)$, is approximated by a piece-wise linear function (see Fig.5) in the log-log domain:

$$N_\psi(f) = \begin{cases} k_1 / |f|^{a_1} & |f| \le f_1 \\ k_2 / |f|^{a_2} & f_1 \le |f| \le f_2 \\ k_3 / |f|^{a_3} & f_2 \le |f| \le f_3 \\ k_4 & f_3 \le |f| \le B/2 \end{cases} \tag{23}$$

In order to simplify the analysis, the phase noise is represented by $\psi(t) = \phi(t) + \varphi(t)$, where $\phi(t)$ is a member of a stationary process with white spectral density (the grey background in Fig.5) and $\varphi(t)$ is a member of a narrow-band, slowly time varying, non-stationary process, with infinite power (for $k_1 > 1$), due to its spectral singularity at $f = 0$. In addition, the two processes are supposed to be independent, and the effects of the two components on the system performance are separately investigated.

We consider first the effect of the white component, for which closed form results can be obtained, by assuming that $\phi(t) << 1$, and that $\phi(t)$ is symmetrically distributed around 0. Let us indicate with P_ϕ the power of $\phi(t)$ and with

$$m_\phi = E\{e^{j\phi_k}\} = E\left\{\sum_h \frac{(j\phi_k)^h}{h!}\right\} \cong E\left\{1 + j\phi_k - \frac{\phi_k^2}{2}\right\} \cong 1 - \frac{1}{2} P_\phi = 1 - \frac{1}{2} k_4 B \tag{24}$$

the mean value of $e^{j\phi_k}$. The samples of $\phi(t)$ are uncorrelated, thus:

$$\sigma_\varepsilon^2 = \sum_{\substack{k=-N_u/2 \\ k\neq 0}}^{k=N_u/2} E\{|\Psi_k|^2\} = \frac{1}{N^2} \sum_{\substack{k=-N_u/2 \\ k\neq 0}}^{k=N_u/2} \sum_m \sum_n E\{e^{j\phi_m} e^{-j\phi_n}\} e^{j2\pi \frac{k(m-n)}{N}} = \frac{1}{N^2} \sum_{\substack{k=-N_u/2 \\ k\neq 0}}^{k=N_u/2} \sum_m \left(1 + m_\phi^2 e^{j2\pi \frac{km}{N}} \sum_{n\neq m} e^{-j2\pi \frac{kn}{N}}\right) =$$

$$= \frac{1}{N^2} \sum_{\substack{k=-N_u/2 \\ k\neq 0}}^{k=N_u/2} \sum_m (1 - m_\phi^2) = \frac{N_U}{N} (1 - m_\phi^2) \cong \frac{N_U}{N} P_\phi = \frac{N_U}{N} k_4 B$$

and:

$$E\{\Psi\} = E\{|\Psi_0|\} = E\left\{\left|\frac{1}{N} \sum_{k=0}^{N-1} e^{j\Psi_k}\right|\right\} \cong \frac{1}{N} E\left\{\sum_{k=0}^{N-1} cos(\psi_k)\right\} = m_\phi$$

In Figure 6, the worsening W is plotted as a function of the SNR for 4 different values of k_4: -90, -93, -100 and -110 dBc/Hz; the curves are obtained using the previous results for the MEDIAN case of $N = 512$, $N_g = 88$

(inclusive of the postamble), N_u = 286 and B=225 Mhz. The data points near the curves are obtained experimentally, using a simulator of the overall system. From the figure we see that the agreement between theoretical and experimental values is good as long as the worsening is moderate. For high values of the worsening the theoretical analysis departs more than 1 dB from the practice. Also we see that a value of k_4<-110 dBc is adequate to ensure negligible performance worsening.

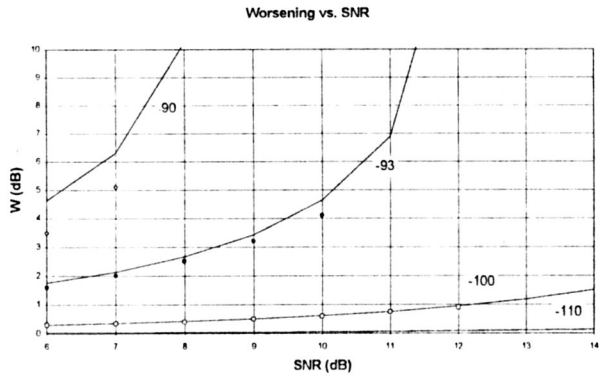

Figure 6 Worsening vs. SNR for different values of k_4.

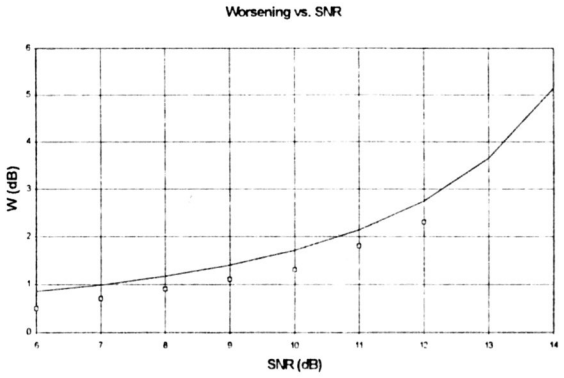

Figure 7 Worsening vs. SNR for LO1.

The effects of the second component are evaluated by measuring σ_ε^2 and $E\{\Psi\}$, based on the assumption that $\varphi(t)$ is gaussian. To this end, a sequence of M independent samples is generated and FFT filtered (with a zero value for $f = 0$), according to the low-pass component of the spectrum represented in Fig.5. The resulting sequence is segmented into M/N groups of N samples; for each group the CSI coefficients are computed by performing a FFT; the sum of the squared CSI coefficients is evaluated according to (21), together with the value of Ψ; the variance σ_ε^2 and $E\{\Psi\}$ are estimated as the mean of these values over all the groups, and used to evaluate the SNR worsening. It is to be noted that, in the frequency domain, the spectrum of the phase noise is sampled with the spacing B/M Hz. This procedure has been carried out (with $M=2^{18}$) using two different phase noise spectrum models, candidate for use in the MEDIAN system, reported in table 1, indicated as LO1 and LO2. The worsening introduced by LO2 is negligible (and this was confirmed by simulations), while LO1 significantly affects the performance: fig.7 plots the theoretical SNR worsening curve obtained for LO1, together with data points obtained by simulation; a maximum difference of 0.3 dB exists between theoretical and simulated results.

Section VI – Conclusions

The present paper presents a complete analysis of analogue filters mismatch both at the transmitter and at the receiver side. Results extend a previous analysis reported in [1].

In addition, the effects of phase noise on QDCPSK-OFDM systems was analyzed. A procedure was devised to evaluate the effects of phase noise on the system SNR. Theoretical results were verified by simulations. The analysis was applied to two oscillators types which are candidate for use in the MEDIAN system; they indicate that only one of the two is suitable for adoption.

References

[1] M. G. di Benedetto, P. Mandarini: "Performance Analysis of a DCQPSK-OFDM modem using analog BB filters", Proc. of ACTS Mobile Summit, Granada, pp. 346-353, Nov. 1996.

[2] W.F. Egan: "Frequency Synthesis by Phase Lock", J. Wiley&Sons, 1981

[3] T. Pollet, M. Van Bladel, M. Moeneclay: "BER sensitivity of OFDM systems to carrier frequency offset and Wiener Phase Noise", IEEE Trans. on Comm. vol. 43, no. 2, pp. 191-193, 1995.

[4] M. Schilpp, W. Sauer-Greff, W. Rupprecht, E. Bogenfeld "Influence of Oscillator Phase noise and Clipping on OFDM for Terrestrial Broadcasting of Digital HDTV", ICC 95, Seattle, USA, pp.1678-1682, 1995.

Acknowledgement

The Median Consortium is greatfully acknowledged. In particular, Dassault Electronique provided the LO spectra.